Chin. J. Astron. Astrophys. Vol. 4 (2004), No. 4, 357–364
(http://www.chjaa.org or http://chjaa.bao.ac.cn)

Chinese Journal of
Astronomy and
Astrophysics

On the Positronium Continuum and 0.511 MeV Line in Solar Flares *

Wei-Qun Gan[1], Jin Chang[1], You-Ping Li[1], Yang Su[1] and L. I. Miroshnichenko[2]

[1] Purple Mountain Observatory, Chinese Academy of Sciences, Nanjing 210008; wqgan@mail.pmo.ac.cn

[2] IZMIRAN, Troitsk, Moscow Region, 142190, Russia

Received 2003 November 18; accepted 2004 January 5

Abstract We have studied the influence of the density of the annihilation region on the positronium continuum. A relation between the ratio $3\gamma/2\gamma$ and the density is explicitly given, with which one can derive directly from the observed $3\gamma/2\gamma$ the density where the annihilation occurs. A unique solution may be found from the observed width of the 0.511 MeV line. We applied the method to three flares observed by GRS/SMM. It is shown that due to the measuring uncertainties in the 0.511 MeV line width, we cannot distinguish a chromospheric source from a coronal source, though both accurately localized. To improve the measuring accuracy of the 0.511 MeV line and the ratio $3\gamma/2\gamma$ will be an important step for a better understanding of the annihilation process in solar flares.

Key words: Sun: flares — Sun: X-rays, gamma-rays

1 INTRODUCTION

Nuclear reactions of accelerated protons and α particles with the ambient medium in solar flares may produce β^+ emitters as well as π^+ mesons. Both β^+ decay and π^+ decay give rise to positrons. The positrons, with an energy around 1 MeV from the β^+ decay and several tens of MeV from the π^+ decay, are slowed down through collisions. When their energy is a few tens of eV, the positrons will either effectively annihilate with the ambient electrons and emit two photons at 0.511 MeV or they form positronium which then annihilates in some way, resulting in two photons at 0.511 MeV and three photons (3γ) at energies smaller than 0.511 MeV. There are four observable quantities related to the annihilation process in solar flares (Gan & Wang 2002): the intensity and width of the 0.511 MeV line, the time variation of the 0.511 MeV line flux, and the 3γ continuum resulting from the positroniums.

The first observations of the 0.511 MeV line in solar flare gamma-ray spectra were made by Chupp et al. (1973), based on the OSO-7 mission. Then with the Gamma-ray Spectrometer (GRS) on the Solar Maximum Mission (SMM) (Forrest et al. 1980) quite a number of gamma-ray flares with obvious 0.511 MeV line emission were observed (Share & Murphy 1997; Vestrand

* Supported by the National Natural Science Foundation of China.

et al. 1999). Among a total 258 gamma-ray flares with an emission above 300 keV (the threshold of the GRS), there are about 67 flares that showed a measurable line emission at 0.511 MeV. The maximum fluence observed by GRS/SMM is 263.8±3.4 photon cm^{-2}, belonging to the X13/3B flare of 1989 October 19, UT 12:56. The 0.511 MeV line fluence for the other flares is mostly less than 10 photons cm^{-2}. The Reuvan Ramaty High Energy Solar Spectroscopic Imager (RHESSI) (Lin 2000) was put into orbit on 2002 February 5. We expect that more flares with a measurable 0.511 MeV line will be observed.

Murphy & Ramaty (1984) calculated the time variation of the 0.511 MeV line for the flares of 1980 June 21 and 1982 June 3. Assuming that the time profile of the production of the positrons is the same as that of the 0.511 MeV line, they showed that for the flare of 1980 June 21, the observation can be very well fitted with a conversion factor from positrons into 0.511 MeV photons of $f_{0.511}$=0.65, an energy spectral index αT of 0.025 in the Bessel function, and a total number of protons above 30 MeV of 7.2×10^{32}. However, for the 1982 June 3 flare, even with αT=0.04, the calculated flux is still much weaker than the observed, suggesting that more positrons are required. Murphy, Dermer & Ramaty (1987) further studied the flare of 1982 June 3. They found that there are two accelerated components: stochastic accelerated particles and diffusive shock-accelerated particles. The former explains the excess emissions of the 4–7 MeV as well as the 2.223 MeV line, while the latter explains the emissions above 10 MeV and the flux variation with time for the 0.511 MeV line. The calculated flux of the 0.511 MeV line can then fit the observations. Following the method of Murphy & Ramaty (1984), Gan & Rieger (1999) studied the X4.7/1B flare of 1988 December 16. Differing from the results obtained by Murphy & Ramaty (1984), Gan & Rieger (1999) showed that in order to fit the observed 0.511 MeV line time profile, the spectral index or $f_{0.511}$ should vary with the time. If so, this means that the annihilation region would change with time during the flare (Gan 2000).

In regard to the width of the 0.511 MeV line and 3γ continuum, so far only Share & Murphy (1997) extracted the line profile and continuum for 19 intense gamma-ray line flares observed with GRS/SMM. Their plots show that the intensity ratio $3\gamma/2\gamma$ can be either much less than 1.0, or about 1.0, or much greater than 1.0. The first two cases, $3\gamma/2\gamma \ll 1.0$ and ~ 1.0, are understandable (Crannell et al. 1976); but the case of $3\gamma/2\gamma \gg 1.0$ is hard to understand, since the ratio has a theoretical maximum at 4.5. We noticed that the flares of this last case are all located close to the solar limb. The strong absorption of Compton scattering might have resulted in an attenuation of the 0.511 MeV line. The formation of the $3\gamma/2\gamma$ ratio has been studied by Share, Murphy & Skibo (1996). Assuming that the ambient medium is fully ionized hydrogen and the density is smaller than 10^{13} cm^{-3}, they obtained a theoretical relationship between the $3\gamma/2\gamma$ ratio and the line width. However, detailed calculations of the ratio as a function of both density and temperature have not been made there. Share & Murphy (2000) reviewed the studies on positron annihilation.

In this paper, we study the dependence of the $3\gamma/2\gamma$ ratio on the density of the annihilation region. Using a flare model atmosphere, we develop an explicit method with which one can easily derive the density and temperature where the annihilation occurs. We shall then present applications of the method to some flares observed with GRS/SMM.

2 THEORETICAL RESULTS

Bussard, Ramaty & Drachman (1979) studied in detail the annihilation process between electrons and positrons. Four ways of annihilations were clarified: direct annihilation between thermal positrons and free electrons (rate $R_{\rm da1}$); direct annihilation between thermal positrons and bounded electrons in hydrogen atoms (rate $R_{\rm da2}$); annihilation via positronium formed by radiative recombination between thermal positrons and free electrons (rate $R_{\rm rr}$), and annihilation via positronium formed by the combination between the thermal positrons and the bounded electrons in neutral hydrogen atoms (rate $R_{\rm ce}$). They calculated the temperature variation of the four rates (per particle). Crannell et al. (1976) studied the probability of a positronium annihilating into 3γ or 2γ as a function of the density. The observed $3\gamma/2\gamma$ ratio seems to be related to the density and the temperature of the annihilation region; however, to explicitly derive the density and temperature from the observed $3\gamma/2\gamma$ ratio is not so clear.

Based on the work of Bussard, Ramaty & Drachman (1979), we can calculate the rate ratio of direct annihilation to the formation of positronium, $R_{\rm da}/R_{\rm ps} = (R_{\rm da1} + R_{\rm da2})/(R_{\rm rr} + R_{\rm ce})$, as a function of the neutral hydrogen density, electron density, and temperature. In order to establish a relationship between the ratio $R_{\rm da}/R_{\rm ps}$ and the density of the annihilation region, we adopted the flare model atmosphere F2 (Machado et al. 1980), which can be taken as a representative of an intense flare. Certainly we can also take other flare models (e.g., Gan & Fang 1987; Gan, Rieger & Fang 1993) which matched real flares; but we adopted the F2 model for a general orientation. We assume that the temperature at the top of the flare loop is 2×10^7K, and that there is an equal pressure distribution in the coronal part of the flare. With these assumptions, we have extended the chromospheric model F2 to the corona, so that we can obtain a definite relationship among the temperature, neutral hydrogen density, total hydrogen density, and electron density. The solid curve in Fig. 1 shows the variation of the $R_{\rm da}/R_{\rm ps}$ ratio with the hydrogen density. This theoretical result, although quantitatively depending on the adopted model atmosphere, may have a general meaning. In Fig. 1 there is a structure between $n_{\rm H} = 10^{13}$ and 10^{14} cm^{-3}, which arises from the electron distribution in the upper chromosphere.

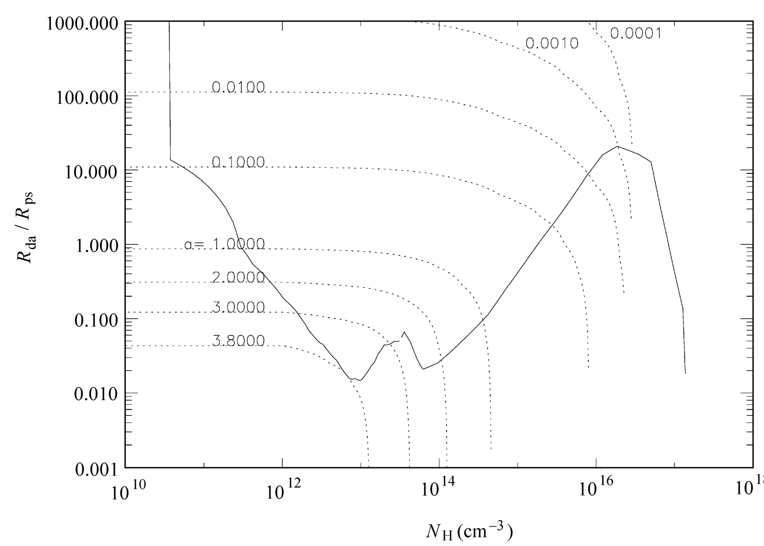

Fig. 1 $R_{\rm da}/R_{\rm ps}$ as a function of the hydrogen density. The solid line is based on the calculations of Bussard et al. (1979), together with a consideration of a flare model atmosphere. The dashed line for a series of $a(= 3\gamma/2\gamma)$ is based on the calculations of Crannell et al. (1976).

Writing $3\gamma/2\gamma = a$, x for the proportion of positrons forming positronium, $1-x$ for the proportion of positrons annihilating directly, and α_1, α_2, and α_3 for the probability of ^{3}Ps decay, ^{1}Ps decay, and the increased free annihilation due to the breakup of ^{3}Ps, respectively, $(\alpha_1+\alpha_2+\alpha_3=1)$, we have

$$a = \frac{3\alpha_1 x}{2(1-x)+2\alpha_2 x+2\alpha_3 x} \equiv \frac{3\alpha_1 x}{2(1-\alpha_1 x)}, \tag{1}$$

that is

$$x = \frac{2a}{\alpha_1(3+2a)}, \tag{2}$$

while

$$\frac{R_{\rm da}}{R_{\rm ps}} = \frac{1-x}{x} \equiv \alpha_1\left(\frac{3}{2a}+1\right) - 1\,. \tag{3}$$

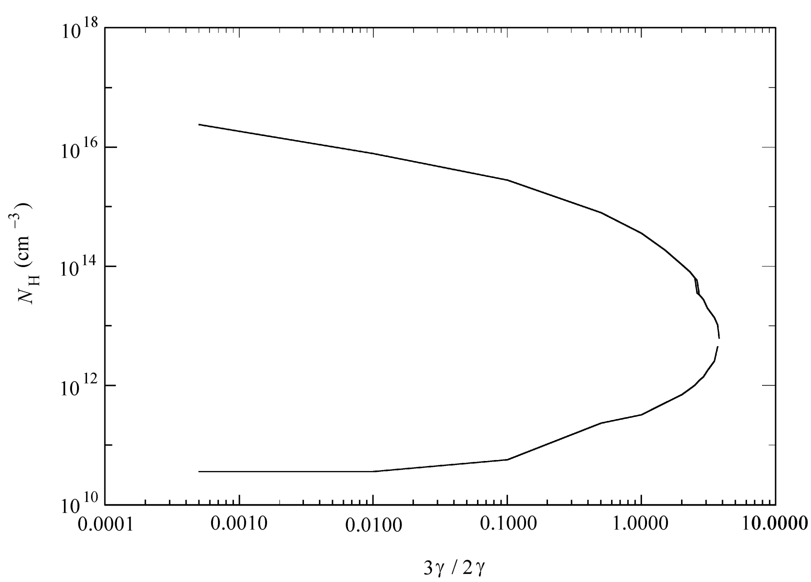

Fig. 2 Theoretical correlation between the ratio $3\gamma/2\gamma$ and the hydrogen density of the annihilation region.

For a given a, we may calculate the variation of $R_{\rm da}/R_{\rm ps}$ with α_1. Referring to the relationship between the density and α_1 (Crannell et al. 1976), we can obtain the variation of $R_{\rm da}/R_{\rm ps}$ with the density shown by the dashed curve in Fig. 1. The point where the solid curve intersects the dashed curve is the solution for a given a, and we obtain for the set of a, the correlation between the density and a shown in Fig. 2. The significance of Fig. 2 is that as long as we know the observed $3\gamma/2\gamma$, we can directly derive the density where the annihilation occurs. Then, for a given flare model atmosphere, we can deduce the temperature, the density of electrons, and the height above the photosphere.

From Fig. 2 we see that there are generally two densities for a given value of $3\gamma/2\gamma$: a lower value corresponding to the region being in the corona, and a higher one corresponding to the region being in the chromosphere. This reflects an uncertainty in determining the density by using only the observed $3\gamma/2\gamma$. The reason for this non-uniqueness is that the dominant region for 2γ production can be either in the corona where few positroniums are formed or in the deep chromosphere where the formed positroniums in triplet state are broken up due to collisions. Within $a = 2.63$ to $a = 2.65$, there are even three densities for a given $3\gamma/2\gamma$, which results from the structure of the distribution of electron density. Figure 2 shows us also that the maximum $3\gamma/2\gamma$ is 3.8, lower than the well-known theoretical value of 4.5 (e.g., Crannell et al. 1976).

Let us take the maximum $3\gamma/2\gamma$ value of 3.8, then the ratio of direct annihilation for positrons is only 4.4%, i.e., there are only 4.4% of positrons annihilating directly. If we use the conversion factor $f_{0.511}$ to represent the 0.511 MeV photons from a positron, the minimum of $f_{0.511}$ is therefore 0.57, a little greater than the widely known value of 0.5 (e.g., Ramaty 1986). Although we have not considered possible absorption due to Compton scattering, this minimum $f_{0.511} = 0.57$ is at least suitable for disk events. As mentioned in Sect. 1, among the 19 flares shown by Share & Murphy (1997) we noticed two with observed $3\gamma/2\gamma \gg 1.0$, which might have resulted from Compton scattering absorption, since both flares are at the solar limb.

3 APPLICATIONS AND DISCUSSION

Share, Murphy & Skibo (1996) gave explicitly the observed $3\gamma/2\gamma$ and width of the 0.511 MeV line for the seven flares studied. Here we take three of them and copy the relevant data in Table 1. The flares taken here are all with averaged $3\gamma/2\gamma$ ratios greater than 0 and with relatively small measuring errors in both the width of the 0.511 MeV line and the $3\gamma/2\gamma$ ratio.

Inserting the observed $3\gamma/2\gamma$ in Table 1 into Fig. 2, we can derive the density of the annihilation region. Together with the flare model atmosphere described in Sect. 2, the corresponding temperature can also be derived. Table 2 lists the derived densities and temperatures, where we use pairs of subscript and superscript to express the error bars.

Table 1 Three GRS/SMM Events with Measured $3\gamma/2\gamma$ and 0.511 MeV Line Width

Flare	Date	Time (UT)	Accum. (s)	Loc.	Imp.	$3\gamma/2\gamma$	Width (keV)
1	3 June 1982	11:42:27	1195	S09E72	X8.0/2B	$1.34^{+0.36}_{-0.36}$	$11.7^{+4.3}_{-11.7}$
2	24 Apr. 1984	23:59:26	1097	S11E45	X13.0/3B	$1.05^{+0.15}_{-0.15}$	$8.0^{+2.6}_{-8.0}$
3	19 Oct. 1989	12:56:39	3260	S25E09	X13.0/3B	$0.4^{+0.15}_{-0.15}$	$10.7^{+2.1}_{-4.7}$

Table 2 The Derived Density and Temperature for 3 GRS/SMM Events

Flare	Density 1 ($\times 10^{14}$ cm^{-3})	Temperature 1 (K)	Density 2 ($\times 10^{11}$ cm^{-3})	Temperature 2 (K)
1	$2.30^{+1.29}_{-0.74}$	$7386.5^{+267.3}_{-297.8}$	$4.35^{+1.27}_{-3.19}$	$6.90^{+4.0}_{-1.47} \times 10^5$
2	$3.16^{+0.92}_{-0.38}$	$7174.0^{+85.7}_{-168.4}$	$3.37^{+0.46}_{-0.4}$	$8.96^{+1.14}_{-1.09} \times 10^5$
3	$9.38^{+4.42}_{-2.12}$	$6482.7^{+150.8}_{-227.8}$	$2.02^{+0.43}_{-0.73}$	$2.52^{+1.75}_{-0.75} \times 10^6$

There are two solutions of the annihilation region for each flare: one is in the corona or upper transition region, the other is in the chromosphere. If we assume that they all originate in the chromosphere, then the annihilation region of flare 3 is in the deepest layer, at about 625 km above the optical thickness τ_{5000}=1. If, on the other hand, we assume that they all originate in the corona, then the annihilation region is in the lower part of the corona, since the upper coronal temperature is around 2×10^7 K in strong solar flares. Two of the three (flares 1 and 2) may even be at the upper transition region.

In order to distinguish the chromospheric origin from the coronal origin, we have to make use of the width of the 0.511 MeV line. It is known that the width of the 0.511 MeV line contains information on the temperature of the annihilation region (e.g., Crannell et al. 1976). For a fully ionized hydrogen medium, i.e, $T > 10^6$ K, the line width due to thermal broadening, written as $1.1(T/10^4)^{1/2}$ (keV), is greater than 11 keV; for a temperature from a few times 10^4 K to 10^6 K, the line width is about $(T/10^4 - 7)^{1/2}$ (keV); for lower temperatures, the line width is from 3 to 5 keV. In the latter two cases, both the temperature and the state of ionization determine the width of the line.

For flare 1, the measured line width implies a range of temperatures smaller than 2.1×10^6 K. Obviously both the chromospheric source and the coronal source for flare 1 in Table 2 satisfy this temperature constraint. For flare 2, the measured line width implies that the temperature should be smaller than 1.2×10^6 K. In comparison with the temperatures of flare 2 in Table 2, the result is the same as for flare 1, i.e., we still cannot distinguish between a chromospheric and coronal source. For flare 3, the measured line width requires a temperature from 4.3×10^5 K to 1.4×10^6 K, while neither of the derived two temperatures in Table 2 is within this range. If a more conservative $\pm2\sigma$ error bar is considered, however, there is an overlap between the temperature derived from the $3\gamma/2\gamma$ and that derived from the width, that is, both the chromospheric source and the coronal source are possible.

So far we have not uniquely determined the annihilation region for any of the three flares studied by using both the observed $3\gamma/2\gamma$ and width of the 0.511 MeV line. One reason is the measuring accuracy of the 0.511 MeV line width. The large error bars mean that we cannot exclude the chromospheric source. Decreasing the error bars of both the line width and the ratio $3\gamma/2\gamma$ will be the key to a unique localization of the annihilation region. On the other hand, there may be some physical reasons involved in this indeterminateness. Taking flare 3 as an example, where the error is not so large and we still cannot get a unique solution. One possibility here is that the two annihilation regions given by the observed $3\gamma/2\gamma$ may both play a role, and that the 0.511 MeV line is a combination of contributions from both. Additional support for this conjecture is that the accumulation time of flare 3 is about 3260 s, long enough to cover the extended phase appearing usually in extremely strong gamma-ray flares (e.g., Rank et al. 2001). At the extended phase, the positrons should come mainly from the π^+-decay with an initial energy of several tens of MeV, which is different from the positrons at the impulsive phase, where most of them come from the β^+-decay with an initial energy of about 1 MeV. However, whether the positrons with different initial energies can react in different regions needs to be studied further, since calculations of the production of excited nuclei (Hua, Ramaty & Lingenfelter 1989) and neutrons (Hua et al. 2002) show that interactions occur in the deeper layer of the atmosphere. The studies on the propagation of positrons might provide some clues. In flare 3, $3\gamma/2\gamma$=0.4 means either x=0.7 for a chromospheric source or x=0.28 for a coronal source. Therefore, the 0.511 MeV line may include four contributions: the direct annihilation (mainly with free electrons) in the corona, the ^{1}Ps (Ps comes mainly from the radiative recombination) decay in the corona, the direct annihilation in the chromosphere, and the increased ^{1}Ps decay (due to the spin flip of ^{3}Ps) in the chromosphere. Further detailed studies should clarify the relative contributions among these four components. We think that this explanation for flare 3 may have some general significance in interpreting other flares, depending on how long the accumulation time is and whether there is an extended phase in which the π^+-decay plays a role. Meanwhile, it seems to be an important topic to extract the temporal behavior of the 0.511 MeV line width as well as the variation of the $3\gamma/2\gamma$ ratio, in order to check our results here.

As a matter of fact, our results here are consistent in some degree with that obtained by Share, Murphy & Skibo (1996), although they did not take into account the detailed influence of the density. Their conclusions are that the GRS/SMM flare measurements are mostly consistent with the ambient material having temperatures ranging from 2×10^5 to 1×10^7 K and densities smaller than 10^{13} cm^{-3}, while the temperature in the annihilation regions might be lower than 10^5 K. Obviously, our results are more refined than theirs.

4 CONCLUSIONS

We have studied the detailed influence of the density of the annihilation region on the $3\gamma/2\gamma$ ratio and presented an explicit relationship between them, so that one can easily derive the density from the observed $3\gamma/2\gamma$. However, the solution is not unique. For a given $3\gamma/2\gamma$, there are usually two solutions for the density. The width of the 0.511 MeV line provides a way to distinguish which density is more suitable. The application of the method to three GRS/SMM events shows that for two of the flares, we cannot distinguish where the annihilation region is, because of the large uncertainties in the measured line width. For the third flare, the one on 1989 October 19, there is a possibility that both regions play a role in the annihilation, one in the corona, the other in the chromosphere.

Obviously, further studies should be based on more advanced observations, in particular, more accurate measurement of the width of the 0.511 MeV line and of the ratio $3\gamma/2\gamma$. It would even be better if the temporal evolution of both the 0.511 MeV line width and the ratio $3\gamma/2\gamma$ can be observed. We expect that RHESSI could provide useful data, so that the annihilation process in solar flares can be better understood. On the other hand, the earlier calculations by Crannell et al. (1976) and Bussard et al. (1979) should be updated by including much of the physics necessary and new cross section data.

Acknowledgements The author would like to express his gratitude to Drs. G. H. Share and E. Rieger for their many helpful comments on the original manuscript. This work is supported in part by the National Natural Science Foundation of China via grants 49990451, 10173027, 10221001, 10333040 and by grant G2000078402 from the Ministry of Science and Technology of China.

References

Bussard R. W., Ramaty R., Drachman R. J., 1979, ApJ, 228, 928
Chupp E. L. et al., 1973, Nature, 241, 333
Crannell C. J., Joyce G., Ramaty R., Werntz C., 1976, ApJ, 210, 582
Forrest D. J. et al., 1980, Solar Phys., 65, 15
Gan W. Q., 2000, In: R. Ramaty, N. Mandzhavidze, eds., High Energy Solar Physics–Anticipating HESSI, ASP Conf. Ser., 206, 439
Gan W. Q., Fang C., 1987, Solar Phys.,107, 311
Gan W. Q., Rieger E., 1999, Solar Phys., 186, 311
Gan W. Q., Rieger E., Fang C., 1993, ApJ, 416, 886
Gan W. Q., Wang D. Y., 2002, High Energy Solar Astrophysics, Beijing: Science Press
Hua X. M., Kozlovsky B., Lingenfelter R. E., Ramaty R., Stupp A., 2002, ApJS, 140, 563
Hua X. M., Ramaty R., Lingenfelter R. E., 1989, ApJ, 341, 516
Lin R. P., 2000, In: R. Ramaty, N. Mandzhavidze, eds., High Energy Solar Physics–Anticipating HESSI, ASP Conf. Ser., 206, 1
Machado M. E., Avrett E. H., Vernazza J. E., Noyes R. W., 1980, ApJ, 242, 336
Murphy R. J., Dermer C. D., Ramaty R., 1987, ApJS, 63, 721
Murphy R. J., Ramaty R., 1984, Adv. Space Res., 4(7), 127
Ramaty R., 1986, In: P. A. Sturrock, T. E. Holzer, D. M. Mihalas, R. K. Ulrich, eds., Physics of the Sun, Volume II: The Solar Atmosphere, Dordrecht: D. Reidel Publishing Company, Chap. 14
Rank G., Ryan J., Debrunner H. et al., 2001, A&A, 378, 1046
Share G. H., Murphy R. J., 1997, ApJ, 485, 409
Share G. H., Murphy R. J., 2000, In: R. Ramaty, N. Mandzhavidze, eds., High Energy Solar Physics–Anticipating HESSI, ASP Conf. Ser., 206, 377
Share G. H., Murphy R. J., Skibo J. G., 1996, In: R. Ramaty, N. Mandzhavidze, X. M. Hua, eds., High Energy Solar Physics, AIP Conf. Proc., 374, 162
Vestrand W. T., Share G. G., Murphy R. J. et al., 1999, ApJS, 120, 409